Trim Analysis of a Classical Octocopter After Single-Rotor Failure

Ariel Walter*, Michael McKay †, Robert Niemiec‡ and Farhan Gandhi§
Center for Mobility with Vertical Lift (MOVE), Rensselaer Polytechnic Institute, Troy, NY, 12180

The performance of an octocopter with single rotor failure is examined in hover and forward flight conditions. The aircraft model uses blade element theory coupled with a finite-state dynamic inflow model to determine rotor aerodynamic forces (thrust, drag, and side-force) and moments (rolling moment, pitching moment, and torque). Failure of various rotors is considered in both flight conditions and an understanding is developed of how the aircraft trims post-failure in terms of multirotor controls defined for the aircraft. In hover, the baseline octocopter trims with all rotors operating at the same rotational speed. When a rotor fails, trim solutions exist that utilize the original reactionless controls of the aircraft to drive the commanded thrust of the failed rotor to zero. The combination of reactionless controls used varies depending on the position of the failed rotor. Post-failure, the primary and reactionless multirotor controls are redefined for each rotor in terms of the original multirotor controls. In forward flight, rotor failure is recovered in a similar manner to the hover case, with additional inputs required to compensate for the rotor hub moments and in-plane forces that were not present in hover. Overall, trim solutions exist for any single rotor failure in both hover and forward flight at 10 m/s. In hover, rotor failure requires an additional 10.7% increase in power to trim, in forward flight this penalty is found to range between 7.7 and 13% depending on the rotor that has failed.

I. Nomenclature

Ω	=	Rotor Rotational Speed
R	=	Rotor Radius
ϕ	=	Aircraft Roll Attitude (Inertial Frame)
θ	=	Aircraft Pitch Attitude (Inertial Frame)
ψ	=	Aircraft Yaw Attitude (Inertial Frame)
u	=	Aircraft x-velocity (Body Frame)
v	=	Aircraft y-velocity (Body Frame)
w	=	Aircraft z-velocity (Body Frame)
p	=	Aircraft Roll Rate (Body Frame)
q	=	Aircraft Pitch Rate (Body Frame)
r	=	Aircraft Yaw Rate (Body Frame)
V_{hub}	=	Hub Velocity
U_T	=	Tangential Wind Velocity
U_P	=	Perpendicular Wind Velocity
λ	=	Inflow Ratio $U_P/\Omega R$
H	=	Rotor Drag
Y	=	Rotor Side Force
T	=	Rotor Thrust
M_x	=	Rotor Roll Moment
M_y	=	Rotor Pitch Moment
M_z	=	Rotor Torque

*Undergraduate Research Assistant, MANE Department, AIAA Student Member.
†Graduate Research Assistant, MANE Department, AIAA Student Member.
‡Ph. D Candidate, MANE Department AIAA Student Member.
§Redfern Chair of Aerospace Engineering, MANE Department, AIAA Associate Fellow.

II. Introduction

Multicopters are gaining popularity in a number of applications including commercial and military operations, as well as hobbyist activities. These aircraft traditionally utilize distributed electric propulsion on multiple fixed-pitch rotors in lieu of traditional collective and cyclic pitch controls found on a typical single main rotor helicopter. This construction makes the aircraft remarkably simple, removing the need for complicated and heavy transmission systems and engines, and replacing the drive train with a system of batteries and wires. To maintain full control of the aircraft, a multicopter must have a minimum of four independent controls. When more than four control effectors are present, the system possesses a redundancy in the generation of forces and moments used to control of the aircraft, which creates the possibility that the aircraft can tolerate the failure of one or more of the control effectors present.

The simplest multicopter, a classical quadcopter as depicted in Fig. 1(a), uses four variable-RPM rotors that correspond to four individual control variables. These four rotor speeds along with the roll and pitch attitude of the aircraft constitute the six trim variables used to solve the six equilibrium equations that determine aircraft trim. However, upon a single rotor failure, the number of control variables is decreased by one, meaning the aircraft is no longer fully controllable. As a result, no complete trim solutions exist for a classical quadcopter after rotor failure, though Mueller and D'Andrea [1] showed that the quadcopter's position could be controlled dynamically by giving up yaw control, even with the failure of up to three rotors. The study gives a method for control of an arbitrary aircraft that has lost the ability to balance torque at an aircraft level.

As previously mentioned, control redundancy is introduced on a multicopter with more than four rotors. Two common configurations with more than four rotors are the classical hexacopter and octocopter, shown in Fig. 1(b) and Fig. 1(c) respectively. When fully operational, these aircraft have 8 and 10 trim variables respectively, given again by the speeds of each rotor as well as the roll and pitch attitudes of the aircraft.

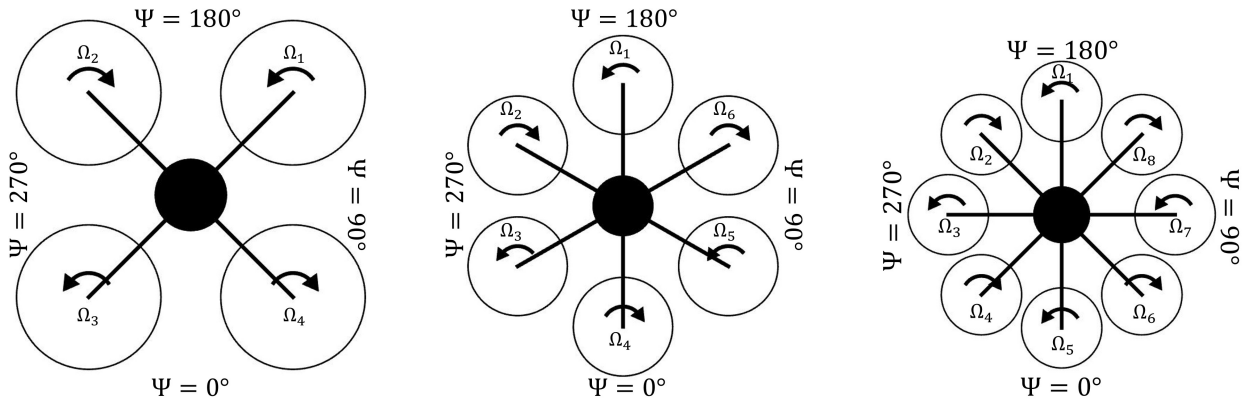

(a) Quadcopter (b) Hexacopter (c) Octocopter

Fig. 1 Three common types of classical multicopters

In theory, these aircraft should be able to maintain trimmed flight even after a rotor failure because of the extra control variables. Facloni and Holzapfel [2] developed an adaptive controller that used no knowledge of the failure type for a hexacopter and demonstrate its effectiveness in simulation. Later, Falconi et al. [3] implemented this control law and demonstrated its performance in outdoor flight testing, showing that a hexacopter can be controlled in the event of rotor failure.

Other groups have explored the ability of a hexacopter to trim and be controlled post-rotor-failure. Schneider et al. [4] define the number of possible failure scenarios that hexacopters and octocopters can tolerate, defined by the set of forces and moments that the aircraft can produce after a rotor fails. The study goes on to propose different arrangements of rotors for each aircraft type that can expand the number of tolerable failure cases, as well as demonstrate use of parametric programming to allocate virtual control inputs and control the aircraft in the event of rotor failure. Achtelik et al. [5] proposed that when a rotor fails on a hexacopter in hover, the rotor diametrically opposite should be spun in either direction (clockwise or counterclockwise) to balance the net torque at the aircraft level.

Marks et al. [6] demonstrate the ability to control an octocopter with a failed rotor. This is with a control allocation matrix that utilizes knowledge of the aircraft rotor arrangement. The pseudo-inverse of this matrix is used to map virtual

control inputs to the actual speeds of the rotors. When a rotor fails, certain elements within the allocation matrix are eliminated, and the pseudo-inverse of this new matrix determines controls for the degraded aircraft. This method is shown to control the aircraft through transient effects as well as drive to a steady state condition.

Prior work on simulating and controlling a multicopter with a failed rotor has used relatively simple physics models. These analyses are typically based on the Ω^2 model, which assumes that the thrust and torque of a rotor are proportional to the square of its rotational speed, with proportionality coefficients obtained through hover testing. The Ω^2-Model also assumes the other forces and moments about the rotor hub are zero. Though adequate in hover, Niemiec and Gandhi [7] show that this is a poor assumption in forward flight.

The model set forth by Niemiec and Gandhi in [7] is based on blade element theory coupled with the Peters-He finite state dynamic inflow model [8] and was used by McKay et al.[9, 10] to conduct a study of hexacopters with single rotor failure. These studies show that with single rotor failure, a classical hexacopter can trim in hover but is not independently controllable about all axes. In forward flight, the authors show that a rotor failure in the front of the aircraft can be trimmed and controlled, but trim is not possible for aft rotor failure. The present study applies strategies similar to those used in [9, 10] to examine single rotor failure of an octocopter in order to examine the effect of additional controls.

As explained by Niemiec and Gandhi [11], the eight individual rotor speed controls for a fully functional octocopter can be transformed into a set of orthogonal multi-rotor controls. The set of multi-rotor controls can be used to produce pure thrust, pitching moment, rolling moment, and torque, rather than the highly coupled response seen with individual rotor controls. Through the modes are applied to the rotor speeds in [11], multi-rotor transformation can also be applied to rotor thrust. Though the results in this study are expressed in terms of rotor thrust, it is important to note that the dynamic equations are still handled in terms of rotor speeds, in order to retain the nonlinear effects, as well as the moments not captured by the Ω^2-Model.

The four primary multi-rotor controls for a fully functional classical octocopter are shown in Fig. 2. The first mode, collective control (T_0, Fig. 2(a)) creates a net thrust by increasing the thrust on all eight rotors by the same amount. Pitch control (T_P, Fig. 2(b)) creates a nose-down pitching moment by increasing the thrust of the rear rotors and decreasing the thrust of the front rotors. Similarly, roll control (T_R, Fig. 2(c)) creates a roll-left moment by increasing the thrust of the rotors on the right and reducing thrust on the left rotors. The final primary control mode, yaw control (T_Y, Fig. 2(d)) creates a nose-left moment by increasing thrust (and torque) on the clockwise-spinning rotors and reducing thrust (and torque) on the counter-clockwise-spinning rotors. The value of the factor k in Figs. 2(b) and 2(c) was found to be $\sin 45^\circ = \cos 45^\circ = \dfrac{1}{\sqrt{2}}$ in Ref[11].

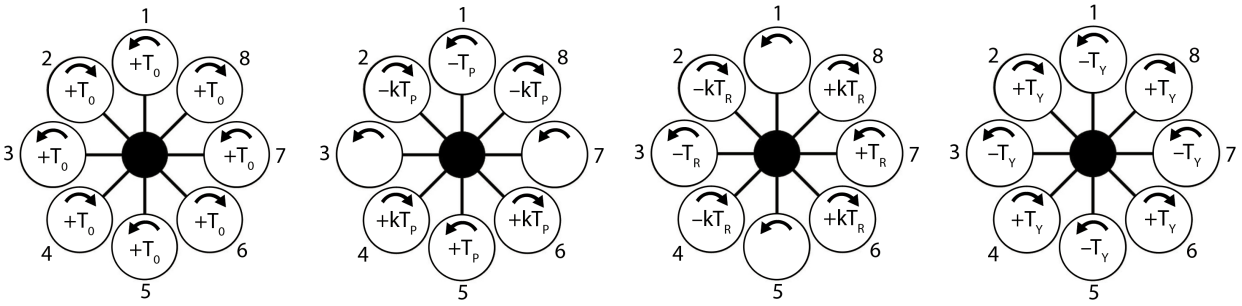

(a) Collective Control (T_0) (b) Pitch Control (T_P) (c) Roll Control (T_R) (d) Yaw Control (T_Y)

Fig. 2 Primary multi-rotor controls for a Classical Octocopter

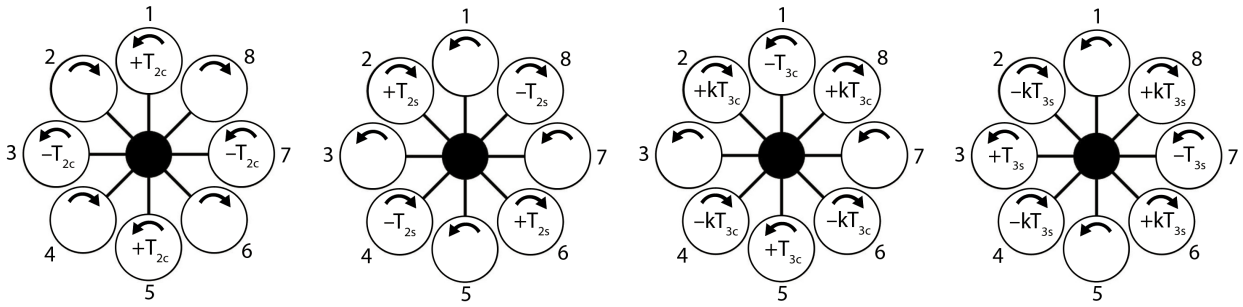

(a) Counterclockwise Lift Share (T_{2c}) (b) Clockwise Lift Share (T_{2s}) (c) Pitch Share (T_{3c}) (d) Roll Share (T_{3s})

Fig. 3 Reactionless multi-rotor controls for a Classical Octocopter

Because an octocopter has four extra controls, four reactionless multi-rotor controls can be defined, as explained in [11]. These reactionless controls produce no net forces or moments at the aircraft level, but instead redistribute the needed forces and moments among the rotors while maintaining equilibrium. The first two reactionless controls, shown in Figs. 3(a) and 3(b), redistribute the thrust produced between the four counter-clockwise-spinning rotors (T_{2c}) or the four clockwise-spinning rotors (T_{2s}), without causing any net forces or moments. The pitch share control (T_{3c}, Fig. 3(d)) redistributes the pitching moment being produced between rotors 1 & 5 and rotors 2, 4, 6, & 8 (Fig. 3(c)). Similar to T_{3c}, the roll share mode (T_{3s}, Fig. 3(d)) redistributes the roll moment being produced between rotors 3 & 7 and rotors 2, 4, 6, & 8. Like the primary modes, the factor k in in Figs. 3(c) and 3(d) was found to be $\frac{1}{\sqrt{2}}$ in Ref. [11]. Conversion from multi-rotor coordinates to individual rotor coordinates is achieved via matrix multiplication, shown in Eq. 1. Each column in the matrix corresponds to a single multi-rotor mode, and each row is associated with a specific rotor.

$$\begin{bmatrix} T_1 \\ T_2 \\ T_3 \\ T_4 \\ T_5 \\ T_6 \\ T_7 \\ T_8 \end{bmatrix} = \begin{bmatrix} 1 & -1 & 0 & -1 & 1 & 0 & -1 & 0 \\ 1 & -\frac{1}{\sqrt{2}} & -\frac{1}{\sqrt{2}} & 1 & 0 & 1 & \frac{1}{\sqrt{2}} & -\frac{1}{\sqrt{2}} \\ 1 & 0 & -1 & -1 & -1 & 0 & 0 & 1 \\ 1 & \frac{1}{\sqrt{2}} & -\frac{1}{\sqrt{2}} & 1 & 0 & -1 & -\frac{1}{\sqrt{2}} & -\frac{1}{\sqrt{2}} \\ 1 & 1 & 0 & -1 & 1 & 0 & 1 & 0 \\ 1 & \frac{1}{\sqrt{2}} & \frac{1}{\sqrt{2}} & 1 & 0 & 1 & -\frac{1}{\sqrt{2}} & \frac{1}{\sqrt{2}} \\ 1 & 0 & 1 & -1 & -1 & 0 & 0 & -1 \\ 1 & -\frac{1}{\sqrt{2}} & \frac{1}{\sqrt{2}} & 1 & 0 & -1 & \frac{1}{\sqrt{2}} & \frac{1}{\sqrt{2}} \end{bmatrix} \begin{bmatrix} T_0 \\ T_P \\ T_R \\ T_Y \\ T_{2c} \\ T_{2s} \\ T_{3c} \\ T_{3s} \end{bmatrix} \tag{1}$$

III. Modeling

A. Aircraft Specifications

A dynamic simulation is implemented to examine the performance of an octocopter based on the AeroQuad Cyclone ARF kit. The aircraft has eight fixed pitch rigid rotors and other aircraft geometry and parameters given in Table 1. These rotors are approximated with a NACA 4412 airfoil at the blade root, with aerodynamic properties and blade geometry linearly interpolated out to a Clark Y airfoil at the blade tip.

B. Rotor Model

The simulation utilizes summation of forces and moments to determine aircraft accelerations. Fuselage drag (modeled as a cylinder), gravity, and aerodynamic forces and moments at the rotor hub are considered, with the latter calculated via blade element theory coupled to a 3×4 (10-state) Peters-He finite state dynamic wake model [8]. Sectional

Table 1 Aircraft Parameters

Parameter	Value
Gross Weight	2 kg
Boom Length	0.3048 m
No. Rotors	8
Rotor Radius	0.1078 m
Tip Airfoil	Clark Y
Tip Chord	0.0087 m
Tip Pitch	11.1°
Root Airfoil	NACA 4412
Root Chord	0.022 m
Root Pitch	21.5°

aerodynamic forces are integrated along the span and about the rotor azimuth to determine hub forces (thrust, drag, side force) and moments (torque, pitching and rolling moment). A detailed explanation of the rotor model used is presented by the authors in [7], and is repeated here for completeness.

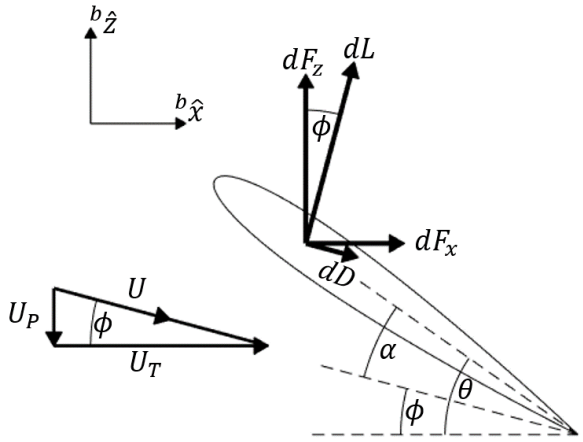

Fig. 4 Cross section of a rotor blade

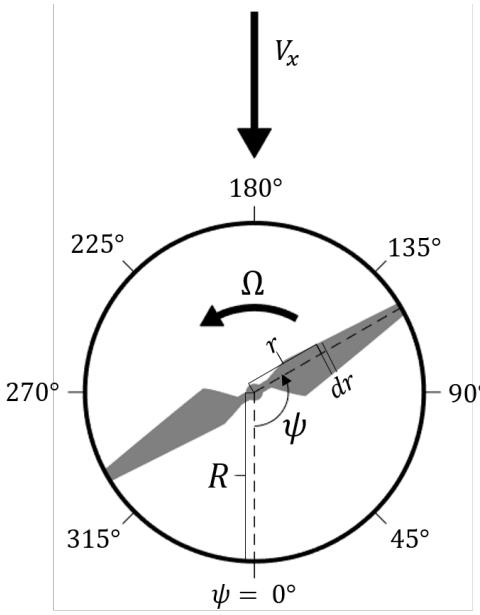

Fig. 5 Top view of rotor in forward flight

At a given blade element, shown in Fig. 4, the local angle of attack can be defined by three parameters; the blade pitch (θ), tangential velocity (U_T, positive leading edge to trailing edge), and perpendicular velocity (U_P, positive downward). The tangential velocity (U_T) is comprised of two components coming from the free stream velocity and the rotational velocity of the rotor. Perpendicular velocity comes from the rotor induced velocity ($v_i = \Omega R \lambda_i$), vertical velocity of the hub, and pitch (r) and roll (p) rotation of the rotor. With these components defined, the tangential and perpendicular velocities are given by Eq. 2.

$$\begin{aligned} U_T &= \Omega r_b + V_{hub,x} \sin\psi_b + (-1)^k V_{hub,y} \cos\psi_b \\ U_P &= \Omega R \lambda_i + V_{hub,z} - (-1)^k r_b p \sin\psi_b - r_b q \cos\psi_b \end{aligned} \tag{2}$$

where r_b and ψ_b (denoted r and ψ in Fig. 5) are the span-wise and azimuthal position of the blade section, as shown in Fig. 5. k is a parameter that takes zero value for counterclockwise spinning rotors and takes a value of 1 for clockwise-spinning rotors. This, as well as the sign reversals on certain rotor-level forces and moments (explained later in this section) allows a single code (which assumes counter-clockwise rotation) to be used for any rotor.

The inflow ratio (λ_i) is defined in the present study using a 3×4 Peters-He [8] finite state dynamic wake model. Using this model λ_i is given by Eq. 3.

$$\lambda_i = \sum_{m=0}^{\infty} \left(\sum_{n=m+1,m+3,\ldots}^{\infty} \phi_n^m(\overline{r}) \left[\alpha_n^m \cos(m\psi_b) + \beta_n^m \sin(m\psi_b) \right] \right) \tag{3}$$

where $\overline{r} = r_b/R$ is the normalized radial position. The dynamics of α_n^m and β_n^m in Eq. 3 are defined by Eq. 4.

$$\begin{aligned} \Omega\{K_m^{nc}\}\{\dot{\alpha}_n^m\} + V[\overline{L}_s]^{-1}\{\alpha_n^m\} &= \frac{1}{2}\{\tau_n^{mc}\} \\ \Omega\{K_m^{nc}\}\{\dot{\beta}_n^m\} + V[\overline{L}_s]^{-1}\{\beta_n^m\} &= \frac{1}{2}\{\tau_n^{ms}\} \end{aligned} \tag{4}$$

Where:

$$\{\tau_n^{0c}\} = \frac{1}{2\pi} \sum_{q=1}^{N_b} \int_0^1 \frac{L}{\rho\Omega^2 R^3} \phi_n^0(\overline{r}) d\overline{r}$$

$$\{\tau_n^{mc}\} = \frac{1}{\pi} \sum_{q=1}^{N_b} \int_0^1 \frac{L}{\rho\Omega^2 R^3} \phi_n^m(\overline{r}) d\overline{r} \cos(m\psi_b)$$

$$\{\tau_n^{ms}\} = \frac{1}{\pi} \sum_{q=1}^{N_b} \int_0^1 \frac{L}{\rho\Omega^2 R^3} \phi_n^m(\overline{r}) d\overline{r} \sin(m\psi_b)$$

These equations are implicitly nonlinear in α_n^m and β_n^m and are solved such that the average values of $\dot{\alpha_n^m}$ and $\dot{\beta_n^m}$ are equal to zero.

With the local flow field for a blade section (defined by U_P and U_T) fully determined by the previous expressions, the local inflow angle (ϕ_i) can be defined via Eq. 5 and the blade section angle of attack is defined by Eq. 6.

$$\phi_i = \tan^{-1} \frac{U_P}{U_T} \tag{5}$$

$$\alpha = \theta - \phi_i \tag{6}$$

Blade elemental lift and drag are then defined (in the wind frame) by the local angle of attack and incident velocities:

$$dL = \frac{1}{2} C_l(\alpha, r_b) \rho (U_T^2 + U_P^2) c dr_b \qquad dD = \frac{1}{2} C_d(\alpha, r_b) \rho (U_T^2 + U_P^2) c dr_b \tag{7}$$

These elemental forces are then rotated by the inflow angle (ϕ_i) to resolve them into the rotor hub frame (normal and tangential to the rotor disk) in Eq. 8.

$$dF_x = dL \sin\phi_i + dD \cos\phi_i \qquad dF_z = dL \cos\phi_i - dD \sin\phi_i \tag{8}$$

These blade elemental forces contribute to the rotor drag (H-force, positive forward), side force (Y-force, positive to the right), and thrust (T, positive downward) as given in Eq. 9. Further, dF_x and dF_z contribute to rotor hub moments as described in Eq. 10. These include the rotor rolling moment (M_x, positive roll-right), pitching moment (M_y, positive nose-up), and rotor torque (M_z, positive nose-right). The parameter k returns, and is zero for a counter-clockwise-spinning rotor and 1 for a clockwise-spinning rotor.

$$\begin{aligned} dH &= -dF_x \sin\psi_b \\ dY &= -(-1)^k dF_x \cos\psi_b \\ dT &= -dF_z \end{aligned} \tag{9}$$

$$\begin{aligned} dM_x &= -(-1)^k dF_z r_b \sin\psi_b \\ dM_y &= -dF_z r_b \cos\psi_b \\ dM_z &= (-1)^k dF_x r_b \end{aligned} \tag{10}$$

These elemental contributions are then integrated along the blade span and averaged about the azimuth, then summed over the number of blades and averaged over one revolution to obtain the average rotor forces and moments. Due to the periodicity of the loads, the expression for average rotor thrust is given by Eq. 11.

$$T = \frac{N_b}{2\pi} \int_0^{2\pi} \int_0^R dT \;\; dr_b \; d\psi_b \tag{11}$$

The remaining rotor forces and moments are determined via similar integrations, substituting the appropriate elemental contributions from Eqs. 9 and 10. Rotor failure is simulated simply by setting the force and moment output of the rotor to zero and ignoring its inflow dynamics.

C. Aircraft Trim

The dynamics of the aircraft are defined by the 6 rigid body equations of motion that describe the aircraft accelerations for three translations and three rotations along and about the body axes. These equations of motion, Eq. 12, are determined by a summation of forces and moments about the center of gravity for the aircraft (beneath the rotor plane at the geometric center of the aircraft). In the derivation, gyroscopic moments are neglected due to the small net angular momentum of the rotors.

$$\begin{aligned}
m\dot{u} &= D_{fuse,x} - g\sin\theta + \sum_{i=1}^{8} H_i & I_{xx}\dot{p} &= -z_{cg}mg\sin\phi\cos\theta + \sum_{i=1}^{8}(M_{x_i} + T_i y_i) \\
m\dot{v} &= D_{fuse,y} - g\sin\phi\cos\theta + \sum_{i=1}^{8} Y_i & I_{yy}\dot{q} &= -z_{cg}mg\sin\theta + \sum_{i=1}^{8}(M_{y_i} + T_i x_i) \\
m\dot{w} &= D_{fuse,z} + g\cos\phi\cos\theta + \sum_{i=1}^{8} T_i & I_{zz}\dot{r} &= \sum_{i=1}^{8}(M_{z_i} + Y_i x_i - H_i y_i)
\end{aligned} \tag{12}$$

Aircraft trim is defined by satisfying the six degree of freedom (3-axis translation and rotation) equilibrium equations, which in turn are defined by setting the equations of motion (Eq. 12) equal to zero, which represents zero acceleration for the aircraft. With four independent controls (i.e. a quadcopter), trim can be solved using the aircraft controls along with the pitch and roll attitudes for the six trim variables. The six nonlinear equations are solved using a Newton-Raphson method as follows. First, the system is defined:

$$f(u) = 0 \tag{13}$$

An initial guess is assumed (u_0), which is updated by the formula:

$$u_{k+1} = u_k - J^{-1} f(u_k) \tag{14}$$

Where J is the Jacobian matrix, defined as:

$$J_{ij} = \left.\frac{\partial f_i}{\partial u_j}\right|_{u=u_k} \tag{15}$$

With more than four independent controls, as is the case for a regular hexacopter or octocopter, there are more trim variables than equations to solve. This results in a non-square Jacobian matrix, therefore J^{-1} is not defined. To circumvent this problem, a pseudoinverse method can be used. In the present study, a Moore-Penrose pseudoinverse (J^+) is used in place of the classical inverse in the Newton-Raphson method:

$$\begin{aligned}
u_{k+1} &= u_k - J^+ f(u_k) \\
J^+ &= J^T (J J^T)^{-1}
\end{aligned} \tag{16}$$

It should be noted that for invertible matrices, the pseudoinverse is identical to the classical matrix inverse. The inflow equations Eq. 4 are solved simultaneously by setting the rate terms to zero and solving for α_n^m and β_n^m for each rotor.

From the trim solution, different key quantities can be extracted aside from the trim controls for the aircraft, including rotor loads and power consumption. The power of an individual rotor can be expressed as the product of its torque and

rotational speed (in steady state), summing these individual rotor contributions will result in the total power for the aircraft.

$$\begin{aligned} P_i &= \tau_i \Omega_i = M_{z_i} \Omega_i \\ P_{AC} &= \sum_{i=1}^{8} P_i \end{aligned} \tag{17}$$

When a rotor fails on the octocopter, seven independent controls remain to trim the aircraft. This leaves a three-dimensional space (corresponding to the three reactionless controls) of possible trim solutions to be explored. To fully explore the space, one control at a time (for a total of three) is parametrically varied (i.e. the speed of one rotor or value of one multi-rotor control), and the unconstrained controls are solved using the pseudoinverse method in the Newton-Raphson framework.

IV. Results

A. Hover Results

1. Rotor 1 Failure

In hover, a fully operational octocopter trims with all eight rotors spinning at identical speeds. Like the classical hexacopter in Refs. [9, 10], the classical octocopter is axisymmetric in hover. As a consequence, post-failure trim solutions are identical, except for a rotation, regardless of which rotor fails. Arbitrarily, consider the failure of rotor 1. If the speed of the other rotors are not changed, there is a net loss of thrust, a nose-down pitching moment, and a nose-left yaw moment as a result of the rotor failure.

The fully operational octocopter would use the primary modes derived in [11] to trim any imbalances. With a rotor failure, these modes no longer produce solely the intended force or moment at the aircraft level. However, the aircraft could be re-trimmed if some combination of the extra controls (which produce no net force or moment for the baseline aircraft) could drive the output of the failed rotor to zero. The T_{2c} and T_{3c} modes defined previously can be used to do this in the case of rotor 1 failure. Given the fact that a combination of these two modes would effectively deactivate the front rotor, the same combination should achieve an equilibrium state for the aircraft in hover after rotor 1 fails. The exact combination of T_{2c} and T_{3c} is given in Eq. 18 where the change in rotor thrusts after failure (ΔT_{hover}) has been normalized by dividing by the thrust produced by each rotor before failure (T_0). The two mode shapes are given again in Eq. 19.

$$\begin{aligned} \frac{\Delta T_{hover}}{T_0} &= c_{2c} T_{2c} + c_{3c} T_{3c} \\ c_{2c} &= -0.51 \quad c_{3c} = 0.49 \end{aligned} \tag{18}$$

Where $\delta T_h over$ is the change in each rotor's thrust after rotor 1 failure using the pseudoinverse method to arrive at a trim solution and T_0 represents the thrust carried by rotor 1 in hover before failure (one-eighth the gross weight). After conversion to multi-rotor coordinates, the values of c_{2c} and c_{3c} are extracted.

$$\begin{aligned} T_{2c} &= \begin{bmatrix} 1 & 0 & -1 & 0 & 1 & 0 & -1 & 0 \end{bmatrix}^T \\ T_{3c} &= \begin{bmatrix} -1 & \frac{1}{\sqrt{2}} & 0 & -\frac{1}{\sqrt{2}} & 1 & -\frac{1}{\sqrt{2}} & 0 & \frac{1}{\sqrt{2}} \end{bmatrix}^T \end{aligned} \tag{19}$$

Positive T_{2c} produces an increase in rotor 1 thrust. By using negative T_{2c} ($c_{2c} < 0$), the thrust ordinarily carried by rotor one is offloaded onto rotors 3 and 7 (rotor 5 thrust is also reduced). Next, the use of T_{3c} redistributes the production of pitching moment away from rotor 1, so positive T_{3c} is used to and redistribute pitching moment to the remaining rotors located off of the aircraft pitching axis (rotors 2, 4, 6, and 8). The use of this mode again reduces the thrust produced by rotor 1, while it increases the thrust carried by rotor 5. Overall, the combination defined in Eq. 18

eliminates the thrust output of the front rotor (capturing the rotor failure), and redistributes its contributions to total aircraft thrust and pitching moment to the remaining operational rotors. The changes imparted on each rotor by the T_{2c} and T_{3c} modes for this octocopter are shown in Table 2.

Table 2 Changes in Thrusts upon Rotor 1 Failure in Hover

Rotor Number	Fully Operational (N)	$-1.26T_{2c}$ (N)	$+1.19T_{3c}$ (N)	Failed Rotor 1 (N)	ΔT (N)
1	2.45	–1.26	–1.19	0	–2.45
2	2.45	0	+0.84	3.29	0.84
3	2.45	+1.26	0	3.72	1.26
4	2.45	0	–0.84	1.61	–0.84
5	2.45	–1.26	+1.19	2.38	–0.08
6	2.45	0	–0.84	1.61	–0.84
7	2.45	+1.26	0	3.72	1.26
8	2.45	0	+0.84	3.29	0.84

The trim solution presented in Table 2 is just one of infinitely many solutions. With seven operational rotors, an octocopter with single rotor failure has a three-dimensional space of trim solutions. If the solution in Table 2 is defined as the origin of this space, then three linearly independent control modes are needed to complete a basis for all possible trim solutions. These three modes must satisfy two additional constraints:

- The control modes must not introduce any net forces or moments at the aircraft level to retain aircraft trim
- They must not utilize rotor 1 (as it is broken)

Two of the original reactionless control modes (T_{2s} and T_{3s}) satisfy these requirements. It is straightforward to verify that these two modes are linearly independent (in fact, they are actually orthogonal to one another with respect to the L_2 inner product). Further, as reactionless modes, they also produce no net forces or moments at the aircraft level. Finally, from Figs. 3(b) and 3(d), these two modes do not use rotor 1. The mode shapes for T_{2s} and T_{3s} are given in Eq. 20. The T_{2s} and T_{3s} vectors correspond to the slopes of the lines in Fig. 6 and Fig. 7, respectively.

$$\begin{aligned} T_{2s} &= \begin{bmatrix} 0 & 1 & 0 & -1 & 0 & 1 & 0 & -1 \end{bmatrix}^T \\ T_{3s} &= \begin{bmatrix} 0 & -1/\sqrt{2} & 1 & -1/\sqrt{2} & 0 & 1/\sqrt{2} & -1 & 1/\sqrt{2} \end{bmatrix}^T \end{aligned} \tag{20}$$

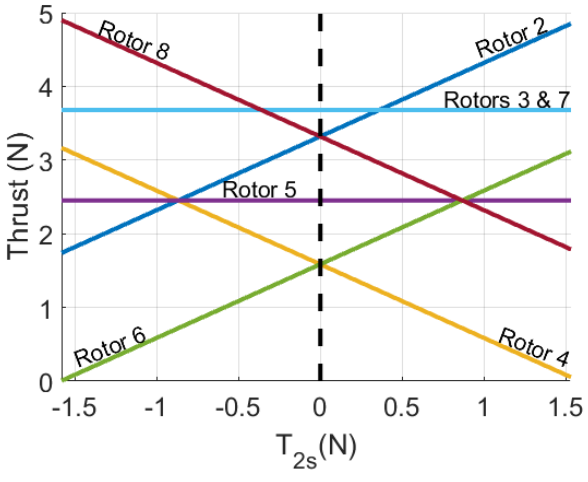

Fig. 6 Family of hover trim solutions with rotor 1 failure corresponding to T_{2s} mode

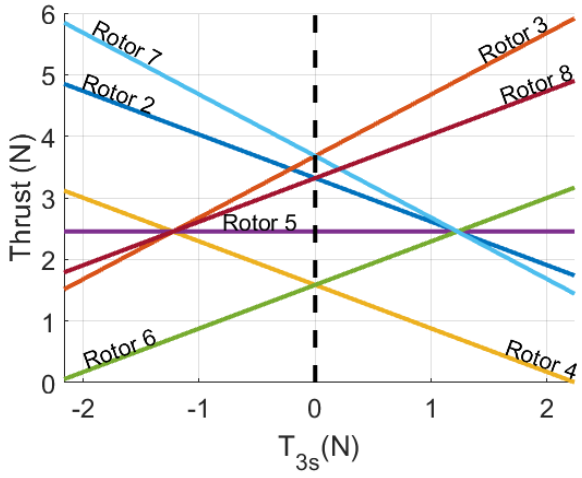

Fig. 7 Family of hover trim solutions with rotor 1 failure corresponding to T_{3s} mode

The family of solutions along the T_{2s} axis are plotted in Fig. 6. Beginning from the pseudoinverse solution, represented by the black dashed line, if the thrust on rotor 2 is increased, then the thrust on rotor 6 is increased by the same amount, to balance rolling and pitching moments. To balance the thrust and torque, the thrust on rotors 4 and 8 are reduced by the same amount. Clearly, the thrust output from rotors 3, 5, and 7 remain unchanged (as would the thrust of rotor 1 if it were operational) with changes in the T_{2s} mode. These results follow directly from the definition of the T_{2s} mode, depicted in Fig. 3.

Given an increase in the T_{3s} mode, rotors 2, 4, 6, and 8 produce a roll-left moment (while remaining balanced in thrust, pitch, and yaw at the aircraft level), and rotors 3 and 7 produce a roll-right moment of equal magnitude (due to their larger moment arms). At the aircraft level, the roll moments cancel. Provided the mode shape defined in Eq. 20 and the graphical representation in Fig. 3, it is clear that increasing the thrust output of rotor 2 is given by a negative T_{3s} input. Therefore, the thrust of rotor 4 should increase by the same amount as rotor 2, while rotors 6 and 8 decrease thrust by the same increment. Also, the thrust of rotor 3 should decrease by the same amount as the increase in rotor 7 thrust (which is a larger increment than rotors 2, 4, 6, and 8). As was the case for the T_{2s} mode, rotor 5 thrust (and rotor 1 thrust) remains unchanged. The solutions along the T_{3s} axis are plotted in Fig. 7, with the pseudoinverse solution represented by the black dashed line.

As previously stated, an octocopter with single rotor failure has 7 independent controls. In a multi-rotor sense, these controls are given by four primary controls and three reactionless controls. The first two reactionless controls have been defined as the T_{2s} and T_{3s} modes and explored in Figs. 6 and 7. The remaining reactionless control is yet to be defined, but can be explored by parametrically varying of rotor 5 thrust (neither T_{2s} nor T_{3s} use rotor 5, so constraining rotor 5 will result in an independent solution space). The family of solutions found by this method is defined by Eq. 21 and is illustrated in Fig. 8.

$$T_{\text{sym}} = \begin{bmatrix} 0 & \frac{\sqrt{2}}{4} & -\frac{1}{2} & -\frac{\sqrt{2}}{4} & 1 & -\frac{\sqrt{2}}{4} & -\frac{1}{2} & \frac{\sqrt{2}}{4} \end{bmatrix}^T \tag{21}$$

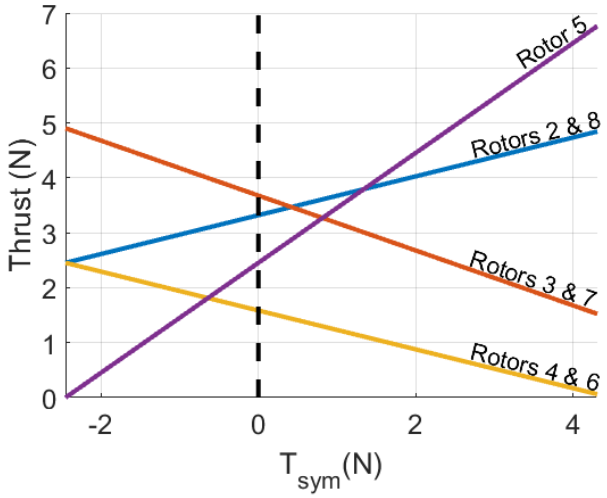

Fig. 8 Family of hover trim solutions with rotor 1 failure corresponding to T_{sym} mode

Along with the T_{2s} and T_{3s} modes discussed so far, the family of trim solutions provided in Fig. 8 defines the last reactionless control mode for the octocopter with rotor 1 failure. The mode shape given in Eq. 21, is equal to slopes of the individual lines in Fig. 8, with the pseudoinverse solution represented by the vertical dashed line.

If the thrust of rotor 5 were to increase with the other four rotors unchanged, it would produce a substantial nose-down pitching moment. To compensate for this, the thrust of rotors 2 and 8 (located forward of the pitching axis) are increased, while rotors 4 and 6 (aft of the pitching axis) produce less thrust. The thrust of rotors 3 and 7 are reduced in order to maintain overall thrust. At each solution in this family, each rotor on the left of the aircraft (2, 3, and 4) has a corresponding rotor on the right of the aircraft (8, 7, and 6) that produces the same thrust. Thus, this set of changes in thrust is referred to as the "symmetric" mode, denoted T_{sym}.

Because T_{sym} is a reactionless mode, it must be contained within the space defined by the original octocopter reactionless modes. Further, it can be shown that it is orthogonal to both T_{2s} and T_{3s}. Therefore, T_{sym} must be a linear combination of only T_{2c} and T_{3c}. The only way to use T_{2c} and T_{3c} without affecting rotor 1 is to use them in a ratio of 1:1 (see Eq. 19). Therefore, Eq. 22 is true, and Fig. 9 represents this equation pictorially.

$$T_{sym} = \frac{T_{2c} + T_{3c}}{2} \tag{22}$$

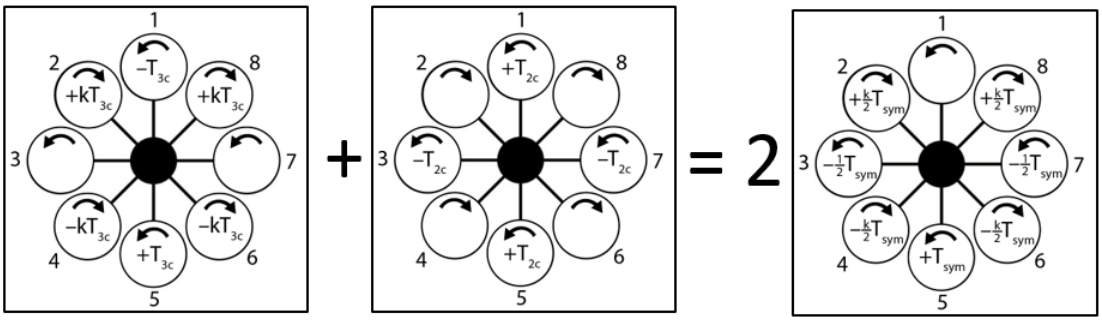

Fig. 9 Reactionless Mode Combination of Symmetric Mode

The aircraft power consumption is a function of the values of the reactionless modes, and can be evaluated. The results are plotted in Fig. 10, which indicates that for best power performance, the reactionless controls should be held at zero, a result that is consistent with the findings given in [11].

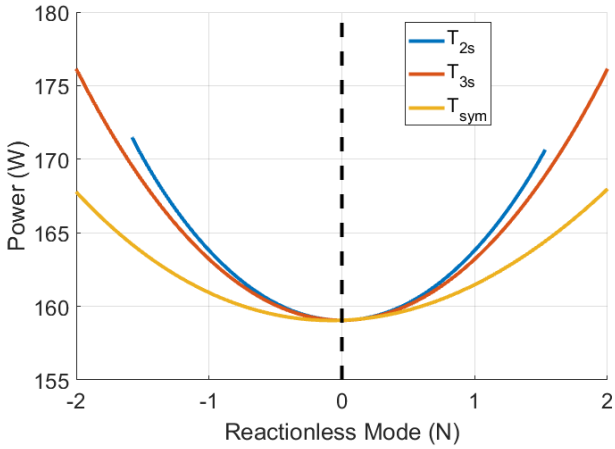

Fig. 10 Power Requirement for Reactionless Modes of Broken Octocopter in Hover

Though the original primary and reactionless control modes from [11] are useful in the analysis of how the aircraft can be trimmed post-failure, they can not be used to control the broken octocopter as a single-input-single-output (SISO) system sense as is the original intention. Because of the failed rotor 1, the primary modes no longer produce decoupled forces and moments when applied. However, new multi-rotor control modes can be defined for the octocopter with rotor failure that utilize different combinations of the remaining seven rotor speeds to produce single axis accelerations at the aircraft level. These new primary modes must satisfy the following:

- They may not use rotor 1
- They must produce only the intended force or moment
- They must be orthogonal to the new reactionless modes

The only primary control on the pristine octocopter that satisfies these constraints is T_R, which will remain unchanged. For the others, a linear combination of the original reactionless control modes that use rotor 1 (T_{2c} and T_{3c}) can be used to modify the original primary mode to satisfy the first constraint. In doing so, the second constraint is automatically satisfied.

Consider the third constraint. By using only T_{2c} and T_{3c}, the new primary mode will automatically be orthogonal to T_{2s} and T_{3s}. Thus, $T_{0_{B1}}$ can be expressed as Eq. 23. By enforcing the third constraint, Eq. 24 implies that T_{2c} and T_{3c} must be used in equal and opposite parts. Finally, by enforcing the first constraint, the first entry in $T_{0_{B1}}$ must be equal to zero (Eq. 25). Solving these two equations simultaneously yields $c_{2c} = -1/2$ and $c_{3c} = 1/2$, so $T_{0_{B1}}$ is defined by Eq. 23. A similar procedure yields the new pitch control (Eq. 26b) and yaw control (Eq. 26c).

$$T_{0_{B1}} = T_0 + c_{2c}T_{2c} + c_{3c}T_{3c} \tag{23}$$

$$\begin{aligned} T_{0_{B1}}^T T_{sym} &= \frac{1}{2}(T_0 + c_{2c}T_{2s} + c_{3c}T_{3c})^T(T_{2c} + T_{3c}) \\ &= \frac{1}{2}\Big(T_0^T(T_{2c} + T_{3c}) + c_{2c}T_{2c}^T(T_{2c} + T_{3c}) + c_{3c}T_{3c}^T(T_{2c} + T_{3c})\Big) \\ &= \frac{1}{2}(c_{2c}T_{2c}^T T_{2c} + c_{3c}T_{3c}^T T_{3c}) \\ &= 2(c_{2c} + c_{3c}) = 0 \\ &\implies c_{2c} = -c_{3c} \end{aligned} \tag{24}$$

$$1 + c_{2c} - c_{3c} = 0 \tag{25}$$

$$T_{0_{B1}} = T_0 + \frac{-T_{2c} + T_{3c}}{2} \tag{26a}$$

$$T_{P_{B1}} = T_P + \frac{T_{2c} - T_{3c}}{2} \tag{26b}$$

$$T_{Y_{B1}} = T_Y + \frac{T_{2c} - T_{3c}}{2} \tag{26c}$$

Taken collectively with the reactionless modes, a new multi-rotor coordinate system with rotor 1 failure can be defined as Eq. 27. With one failed rotor, one row of this transform is entirely zeros, while the seven columns represent the new primary and reactionless modes, of which there is one fewer, due to the loss of rotor 1.

$$\begin{bmatrix} T_1 \\ T_2 \\ T_3 \\ T_4 \\ T_5 \\ T_6 \\ T_7 \\ T_8 \end{bmatrix} = \begin{bmatrix} 0 & 0 & 0 & 0 & 0 & 0 & 0 \\ 1 + \frac{\sqrt{2}}{4} & -\frac{3\sqrt{2}}{4} & -\frac{1}{\sqrt{2}} & 1 - \frac{\sqrt{2}}{4} & \frac{\sqrt{2}}{4} & 1 & -\frac{1}{\sqrt{2}} \\ \frac{3}{2} & -\frac{1}{2} & -1 & -\frac{3}{2} & -\frac{1}{2} & 0 & 1 \\ 1 - \frac{\sqrt{2}}{4} & \frac{3\sqrt{2}}{4} & -\frac{1}{\sqrt{2}} & 1 + \frac{\sqrt{2}}{4} & -\frac{\sqrt{2}}{4} & -1 & -\frac{1}{\sqrt{2}} \\ 1 & 1 & 0 & -1 & 1 & 0 & 0 \\ 1 - \frac{\sqrt{2}}{4} & \frac{3\sqrt{2}}{4} & \frac{1}{\sqrt{2}} & 1 + \frac{\sqrt{2}}{4} & -\frac{\sqrt{2}}{4} & 1 & \frac{1}{\sqrt{2}} \\ \frac{3}{2} & -\frac{1}{2} & 1 & -\frac{3}{2} & -\frac{1}{2} & 0 & -1 \\ 1 + \frac{\sqrt{2}}{4} & -\frac{3\sqrt{2}}{4} & \frac{1}{\sqrt{2}} & 1 - \frac{\sqrt{2}}{4} & \frac{\sqrt{2}}{4} & -1 & \frac{1}{\sqrt{2}} \end{bmatrix} \begin{bmatrix} T_0 \\ T_P \\ T_R \\ T_Y \\ T_{sym} \\ T_{2s} \\ T_{3s} \end{bmatrix}_{B1} \tag{27}$$

2. Other Rotor Failure

Should a rotor other than the front rotor fail, the aircraft response will be different according to the position of the failed rotor, though the end result is identical except for a rotation. It was observed that when rotor 1 failed, the aircraft compensated by use of the reactionless controls T_{2c} and T_{3c} to drive the commanded thrust output of rotor 1 to zero by offloading its thrust and pitching moment contributions amongst the remaining seven functional rotors on the aircraft. For rotor 1 failure, this was done according to the expression given in Eq. 18, with negative c_{2c} input and positive c_{3c} input.

A similar aircraft response would occur for the failure of rotor 5 in hover, with the T_{2c} mode used to redistribute the thrust from rotor 5 to rotors 3 and 7 along with the T_{3c} mode to correct the pitching moment on the aircraft. The values of these inputs will be the same between rotor 1 and rotor 5 failure, but the sign of the c_{3c} input will be switched in order to account for the different direction of pitching moment that arises when rotor 5 fails compared to rotor 1.

Failure of either rotor 3 or 7 would be characteristically similar to that of rotors 1 and 5, with the primary difference being in the use of T_{3s} rather than T_{3c} to correct the aircraft moment. Because rotors 3 and 7 are located 90° away from the front and aft rotors, the loss of either rotor results in a net rolling moment, which is redistributed using the T_{3s} mode, rather than the T_{3c} mode that was used with the pitching moment correction for rotor 1 or 5 failure. To compensate the failure of rotor 3, the aircraft would use a positive input of c_{2c} to correct the aircraft thrust, along with a negative c_{3s} input for the aircraft rolling moment. The combination of these inputs would be such that the commanded thrust of rotor 3 is zero. For rotor 7 failure, the compensation would be similar, but use positive c_{3s} because of the opposite direction of aircraft rolling moment.

Failure of the remaining four rotors is slight more complicated than those discussed to this point. Failure of rotor 2, 4, 6, or 8 results in a net thrust loss, which can be corrected by use of the T_{2s} mode, as well as an imbalance in both aircraft pitch and roll moment. To this end, the compensation for failure of one of these rotors would require use of 3 reactionless controls to drive the aircraft to a new equilibrium state. The relative signs of the control inputs in each case is given in Table 4.

Naturally, the primary control modes will be redefined for each case of rotor failure as well. This redefinition would be done in a similar manner to the case of rotor 1 failure, but with different combinations of the original reactionless modes in order to arrive at a set of decoupled control modes for the thrust and moments of the aircraft.

Take, for example, the case of rotor 5 failure. The new primary control modes that produce thrust, pitching moment, and torque for the aircraft are defined by Eq. 28a (roll control remains identical to the baseline case as it did for failure of rotor 1).

$$T_{0_{B5}} = T_0 + \frac{-T_{2c} - T_{3c}}{2} \tag{28a}$$

$$T_{P_{B5}} = T_P + \frac{-T_{2c} - T_{3c}}{2} \tag{28b}$$

$$T_{Y_{B5}} = T_Y + \frac{T_{2c} + T_{3c}}{2} \tag{28c}$$

Again, the new control modes are written as a sum of the original control mode along with a linear combination of the original reactionless controls that affect the failed rotor. These reactionless controls are used to modify the original primary input such that they do not include the failed rotor. This has the effect of offloading the output of the failed rotor onto the remaining functioning rotors. The signs on each of the terms associated with the reactionless modes are such that the effect each primary mode has on the failed rotor approaches zero. For example, both T_0 and T_P normally increase the thrust on rotor 5 (Figs. 2(a) and 2(b)), as do T_{2c} and T_{3c} (Figs. 3(a) and 3(c)). Therefore, both of these reactionless modes are subtracted from the primary modes, as shown in Eq. 28a. The yaw mode T_Y, on the other hand, ordinarily reduces the thrust on rotor 5 (Fig. 2(d)), and so T_{2c} and T_{3c} are added to the yaw mode. After applying the reactionless control modes, the failed rotor does not participate by the new primary modes, reflecting the fact that it has failed.

Comparing Eqs. 26 and 28, the equations have identical terms except for sign differences, which occur when the sign of either the original primary control or reactionless control effect on the failed rotor changes. For example, T_P has opposite effects on rotors 1 and 5, while T_{2c} has the same effect on these rotors. Therefore, the sign on the T_{2c} term in Eqs. 26b and 28b have opposite sign. That is, T_{2c} is added to T_P in Eq. 26b and subtracted from T_P in Eq. 28b. Since T_{3c} (like T_P) has an opposite effect on both rotors 1 and 5, the T_{3c} terms in Eqs. 26b and 28b have the same sign.

The primary controls can be redefined in the case of any single rotor failure, with differences being in the combination of original reactionless controls used to remove the impact of the new primary modes on the failed rotor. In the case of rotor 1 or rotor 5 failure, it was observed that T_{2c} and T_{3c} were used to modify the original primary control modes because these original reactionless controls can impart changes on the failed rotor command inputs. If the failure of rotor 3 is considered, T_{3c} is not a viable reactionless control to use anymore in modifying the original primary controls as it does not affect the failed rotor (Fig. 3(c)). However, the modification of the original primary control modes takes a similar form to that of rotors 1 and 5 (Eq. 29).

$$T_{0_{B3}} = T_0 + \frac{T_{2c} - T_{3s}}{2} \tag{29a}$$

$$T_{R_{B3}} = T_R + \frac{-T_{2c} + T_{3s}}{2} \tag{29b}$$

$$T_{Y_{B3}} = T_Y + \frac{T_{2c} + T_{3s}}{2} \tag{29c}$$

Because rotor 3 is positioned at $\psi_3 = 270°$, the only reactionless controls that can be used to modify the original primary modes are T_{2c} and T_{3s} (see Fig. 3) . As T_R remained unchanged for the case of rotor 1 and rotor 5 failure because the original primary mode did not utilize the failed rotor, T_P is unchanged for the case of rotor 3 failure (as well as rotor 7 failure). Again, the terms associated with the original reactionless controls in Eq. 29 serve to reduce the effect of the new primary mode on the failed rotor. Results for rotor 7 failure are not presented here, but the expression for the new primary control modes in that case will simply have differently signed terms in accordance with the discussion of rotor 1 and rotor 5 failure cases.

Rotors 1, 3, 5, and 7 are all located such that their thrust commands are changed only by two of the four original reactionless controls. When the even rotors are considered, it is clear that the T_{2s}, T_{3c}, and T_{3s} modes all influence the thrust of these rotors. Following from previous results, these three reactionless controls will be used in combination to redefine the primary control modes for the aircraft in the event of rotor failure. The new primary control modes in for rotor 2 failure are given in Eq. 30.

$$T_{0_{B2}} = T_0 + \frac{1}{2}\big(- T_{2s} + k(-T_{3c} + T_{3s})\big) \tag{30a}$$

$$T_{P_{B2}} = T_P + \frac{1}{2}\left(kT_{2s} + \frac{T_{3c} - T_{3s}}{2}\right) \tag{30b}$$

$$T_{R_{B2}} = T_R + \frac{1}{2}\left(kT_{2s} + \frac{T_{3c} - T_{3s}}{2}\right) \tag{30c}$$

$$T_{Y_{B2}} = T_Y + \frac{1}{2}\big(- T_{2s} + k(-T_{3c} + T_{3s})\big) \tag{30d}$$

Recall that k has previously been defined as $1/\sqrt{2}$. In the case of rotor 2 failure (and by extension 4, 6, and 8), all of the primary control modes are redefined. This is because the all original primary modes (Fig. 2) impact this rotor. In each redefinition, the sign of the original reactionless modes corresponds again to the effect that mode has on rotor 2. That is, each reactionless mode is used to drive the commanded thrust of the failed rotor toward zero. The signs and relative magnitudes of each redundant mode used to redefine the primary controls are given in Tbl. 3 for the odd-numbered rotors and Tbl. 4 for the even-numbered rotors. If the pseudoinverse method is used, the resulting solution is very near the derived solutions (Compare Tbl. 3 to Eq. 18

Table 3 Reactionless Control Input Signs for Odd Rotor Failure

Failed Rotor	c_{2c}	c_{3c}	c_{3s}
1	−0.5	+0.5	0
3	+0.5	0	−0.5
5	−0.5	−0.5	0
7	+0.5	0	+0.5

Table 4 Reactionless Control Input Signs for Even Rotor Failure

Failed Rotor	c_{2s}	c_{3c}	c_{3s}
2	– 0.5	– 0.3536	+ 0.3536
4	+0.5	+ 0.3536	– 0.3536
6	–0.5	+ 0.3536	– 0.3536
8	+0.5	– 0.3536	– 0.3536

B. Forward Flight Results

In hover, the octocopter experiences no in-plane velocity, which means that the rotors see only an axisymmetric induced flow moving through the disk axially. This flow field results in the rotors generating only a net thrust and torque from the blade sectional lift and drag–no net in-plane forces (drag and side force) or moments (roll and pitch) are generated in this condition. However, in forward flight, freestream velocity travelling from rotor 1 to rotor 5, as in Fig. 11, the flow at the rotor disk is non-axisymmetric, primarily as a result of advancing and retreating side effects, which cause changes in the induced inflow distribution on the rotor disk. The variation in local flow field results in net in-plane forces and hub moments for each of the rotors, which are transmitted to the aircraft. Most importantly, there is a net nose-up pitching moment [7] which must be compensated by T_P (so that rotors 4, 5, and 6 produce more thrust than rotors 2, 1, and 8, respectively) to maintain the nose-down attitude necessary for forward flight.

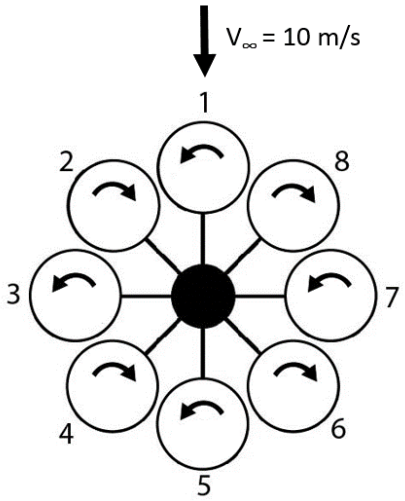

Fig. 11 Octocopter in Forward Flight

In hover, a single rotor could be chosen arbitrarily for analysis because all rotors operated identically. In forward flight, however, the rotors contribute significantly different forces and moments depending on their location on the aircraft. This means each rotor failure must be considered individually in forward flight in order to fully examine the performance of the aircraft post-failure.

1. Failure of Rotor 1

When fully operational, rotor 1 produces a net thrust, drag, and small negative (leftward) side force. The thrust induces a positive (nose-up) pitch moment and the side force induces a small negative (nose-left) yaw moment about the aircraft center of gravity. Additionally, rotor 1 produces a negative (roll-left) roll moment, positive (nose-up) pitch moment, and positive (nose-right) yaw moment about its hub (due to the aforementioned asymmetries).

Upon the failure of rotor 1, the aircraft trims in largely the same way it did in hover–by using T_{2c} to shift lift onto rotors 3 and 7, while using T_{3c} to recover the pitching moment. Like in hover, the application of negative T_{2c} and positive T_{3c} control modes is used to recover thrust and pitching moment lost from rotor 1 failure. However, the use of T_{2c} and T_{3c} creates an imbalance in rolling moment and yaw moment, the latter of which is due to side-force-induced moments lost on rotor 1. Thus, the aircraft is in a near-trim state, with only a small rolling moment and yaw moment to recover using T_R and T_Y, respectively, as shown in Eq. 31. This solution is also power-optimal, and the changes in rotor thrust are detailed in Tbl. 5.

$$\begin{gathered}\frac{\Delta T_{B1}}{T_1} = c_{2c}T_{2c} + c_{3c}T_{3c} + c_R T_R + c_Y T_Y \\ c_{2c} = -0.50 \quad c_{3c} = 0.48 \quad c_R = 0.01 \quad c_Y = 0.02\end{gathered} \tag{31}$$

Table 5 Changes in Thrusts with Rotor 1 Failure in Forward Flight *

Rotor Number	Fully Operational (N)	Failed Rotor 1 (N)	$-1.14T_{2c}$	$+1.09T_{3c}$	ΔT_{B1} (N)
1	0	2.27	–1.14	–1.09	–2.27
2	3.14	2.34	0	+0.77	0.80
3	3.60	2.51	+1.14	0	1.08
4	1.96	2.70	0	–0.77	–0.74
5	2.68	2.77	–1.14	+1.09	–0.10
6	1.98	2.70	0	–0.77	–0.72
7	3.64	2.51	+1.14	0	1.12
8	0.82	2.34	0	+0.77	0.82

* Columns 4 and 5 do not sum to column 6 due to the use of T_R and T_Y for trim

2. Failure of Rotor 5

As was the case in hover, rotor 5 failure in forward flight is characteristically similar to rotor 1 failure. Again, T_{2c} and T_{3c} are used to redistribute the lost thrust and pitching moment contributions from the failed rotor, with small inputs for correction of roll and yaw imbalance from the rotor in-plane forces and hub moments. Equation 32 presents the inputs required to restore equilibrium for the case of rotor 5 failure in forward flight.

$$\begin{gathered}\frac{\Delta T_{B5}}{T_5} = c_{2c}T_{2c} + c_{3c}T_{3c} + c_R T_R + c_Y T_Y \\ c_{2c} = -0.53 \quad c_{3c} = -0.50 \quad c_R = 0.01 \quad c_Y = -0.03\end{gathered} \tag{32}$$

Comparing this expression to that given for rotor 1 failure (Eq. 31), it can be observed that the input magnitudes are generally similar to the previous case. The sign of the T_{3c} input, however, is inverted compared to the rotor 1 failure case, which can be attributed to the oppositely signed pitch moment from rotor 5 relative to rotor 1. Finally, as was the case for rotor 1 failure, small T_R and T_Y inputs are needed to correct for the imbalance from rotor 5 hub roll moment and induced yaw moment, the latter of which is oppositely signed, as the lost side force (which is in the same direction as rotor 1) is on the opposite side of the aircraft.

3. Failure of Rotor 3 or 7

Similar to hover, failure of rotor 3 or 7 is compensated primarily through use of T_{2c} and T_{3s}, with some additional input to correct for any other imbalances at the aircraft level from forward flight effects. Equation 33, which shows the change in rotor thrust when rotor 3 fails, reflects this, primarily using T_{2c} to redistribute aircraft thrust and T_{3s} to redistribute the rolling moment for the aircraft. In losing rotor 3, the aircraft will see a small imbalance from the hub rolling moment of that rotor. Like rotors 1 and 5, the in-plane forces induce yaw moments on the aircraft. However, for rotors 3 and 7, it is drag that induces yaw, rather than side-force, which is significantly smaller. As such, the yaw compensation is greater after rotor 3 is lost is greater than when either rotor 1 or 5 is lost.

$$\begin{gathered}\frac{\Delta T_{B3}}{T_3} = c_{2c}T_{2c} + c_{3s}T_{3s} + c_R T_R + c_Y T_Y \\ c_{2c} = 0.46 \quad c_{3s} = -0.45 \quad c_R = 0.01 \quad c_Y = 0.07\end{gathered} \tag{33}$$

Rotor 7 failure is again qualitatively similar to failure of rotor 3, with a sign change associated with the T_{3s} input due to the different direction of roll moment normally affected by rotor 7 (Eq. 34). Equation 34 also shows a similar T_R input to balance the loss of rotor 7 hub rolling moment (which acts in the same direction as rotor 3, hence the same sign), and an oppositely signed T_Y input corresponding to the opposite direction torque (relative to rotor 3) that results from rotor 7 drag.

$$\begin{gathered}\frac{\Delta T_{B7}}{T_7} = c_{2c}T_{2c} + c_{3s}T_{3s} + c_R T_R + c_Y T_Y \\ c_{2c} = 0.56 \quad c_{3s} = 0.51 \quad c_R = 0.01 \quad c_Y = -0.07\end{gathered} \tag{34}$$

A key difference between Eqs. 33 and 34 is the magnitude of the T_{2c} and T_{3s} terms; in the case of rotor 7 failure these terms are noticeably larger than for rotor 3 failure. To explain this, consider the T_Y input between the two cases. Positive T_Y input decreases the commanded thrust of rotors 3 and 7, whereas a negative input will increase the thrust commanded (Fig. 2(d)). As previously discussed, the aircraft torque induced by the drag of rotor 3 and rotor 7 act to yaw the aircraft in opposite directions, correspondingly changing the sign of the T_Y input required to return the aircraft to equilibrium. Consequently, the magnitude of inputs from T_{2c} and T_{3s} required to drive the commanded thrust of the failed rotor to zero is different between the two cases. Because rotor 7 failure requires a negative T_Y input, the thrust command for rotor 7 is increased (relative to the rotor 3 failure case), which must be reduced by larger T_{2c} and T_{3s} inputs.

4. Failure of Rotor 2 or 8

Failure of an even numbered rotor in hover involved the use of three of the original reactionless modes to recover aircraft equilibrium because rotors 2, 4, 6, and 8 all impact both the roll and pitch moments for the aircraft. In forward flight, recovery from failure still involves the use of the same three modes (T_{2s}, T_{3c}, and T_{3s}). Roll (T_R) and yaw (T_Y) inputs are also required due to the rotor in-plane forces and hub moments as described in previously.

First, consider the case of rotor 2 failure (Eq. 35).

$$\begin{gathered}\frac{\Delta T_{B2}}{T_2} = c_{3c}T_{3c} + c_{2s}T_{2s} + c_{3s}T_{3s} + c_R T_R + c_Y T_Y \\ c_{3c} = -0.36 \quad c_{2s} = -0.54 \quad c_{3s} = 0.35 \quad c_R = -0.01 \quad c_Y = 0.04\end{gathered} \tag{35}$$

T_{2s}, T_{3c}, and T_{3s} are used for the same purpose as in the hover case, with the addition of T_R and T_Y to account for the rotor hub rolling moment and aircraft yaw moment induced by rotor in-plane forces. Note that the T_R input is oppositely signed relative to rotor 1, 3, 5, and 7 failure because the hub rolling moment on the even (clockwise-spinning) rotors acts in the opposite direction.

On the other side of the aircraft, failure of rotor 8 is recovered in a similar manner to rotor 2, with a sign change for the T_{2s} term due to the impact the reactionless mode has on rotor 8 versus rotor 2 (Eq. 36).

$$\begin{gathered}\frac{\Delta T_{B8}}{T_8} = c_{3c}T_{3c} + c_{2s}T_{2s} + c_{3s}T_{3s} + c_R T_R + c_Y T_Y \\ c_{3c} = -0.32 \quad c_{2s} = 0.47 \quad c_{3s} = -0.32 \quad c_R = -0.01 \quad c_Y = -0.07\end{gathered} \tag{36}$$

The differences between rotor 8 and rotor 2 failure are similar to the difference between rotor 3 and rotor 7 failures. That is, rotors 2 and 7 have a larger input for the reactionless controls relative to rotors 8 and 3, respectively. This is a consequence of the yaw input (T_Y) that is required to restore yaw equilibrium for the aircraft. In the case of rotor 7 failure, the T_Y input required to restore yaw equilibrium commands an increase in the failed rotor thrust, which in turn requires larger inputs from the reactionless controls to drive its thrust to zero. In the case of rotor 8 failure, the T_Y command is negative (for rotor 2 failure it was positive). This negative T_Y commands an decrease in rotor 8 thrust, which is compensated by a smaller input of T_{2s}, T_{3c}, and T_{3s}.

5. Failure of Rotor 4 or 6

Failure of rotor 4 or 6 is nearly identical to failure of rotor 2 or 8. The primary difference between these two sets of cases is the change of sign between the T_{3c} term used to return the aircraft to pitch equilibrium, which is simply due to the location of the 4-6 rotor pair relative to the 2-8 pair. The combination of controls that return the aircraft are provided for rotor 4 failure in Eq. 37 and for rotor 6 failure in Eq. 38.

$$\begin{gathered}\frac{\Delta T_{B4}}{T_4} = c_{3c}T_{3c} + c_{2s}T_{2s} + c_{3s}T_{3s} + c_R T_R + c_Y T_Y \\ c_{3c} = 0.36 \quad c_{2s} = 0.55 \quad c_{3s} = 0.36 \quad c_R = -0.01 \quad c_Y = 0.06\end{gathered} \tag{37}$$

$$\begin{gathered}\frac{\Delta T_{B6}}{T_6} = c_{3c}T_{3c} + c_{2s}T_{2s} + c_{3s}T_{3s} + c_R T_R + c_Y T_Y \\ c_{3c} = 0.33 \quad c_{2s} = -0.49 \quad c_{3s} = -0.34 \quad c_R = -0.01 \quad c_Y = -0.03\end{gathered} \tag{38}$$

Comparing the failure case of rotor 4 against rotor 6, the same trends exist as in the previous section. That is, the sign of the T_{2s} mode changes sign and the rotor that requires negative T_Y input (rotor 6 failure) also requires smaller magnitude inputs in the original reactionless modes to restore aircraft equilibrium.

C. Effects of Rotor Failure on Power

Retrimming the aircraft after a single rotor failure in hover results in a 10.7% increase in the power consumption of the octocopter, due to the need for the remaining functional rotors speeding up in order to recover trim equilibrium for the octocopter. Though the total thrust remains constant, the total power increases because the disk loading for the aircraft increases overall (less functional disk area). Additionally, the individual rotors do not all operate at the same disk loading, which further increases the required power. Due to the axisymmetry of the octocopter, this is true regardless of which rotor fails.

In forward flight, the increase in power consumption post-failure is different depending on which rotor has failed, as each rotor provides a unique contribution to the total aircraft load, and so the aircraft trims differently depending on which rotor fails. Table 6 and Fig. 12 give the total power required for each of the eight possible single-rotor failure cases at a flight speed of 10 m/s, relative to the pristine octocopter at the same speed.

Table 6 Change in Power with Broken Rotor in Forward Flight

Broken Rotor	1	2	3	4	5	6	7	8
Percent Increase in Power	8.0	9.5	8.7	13	13	11	12	7.7

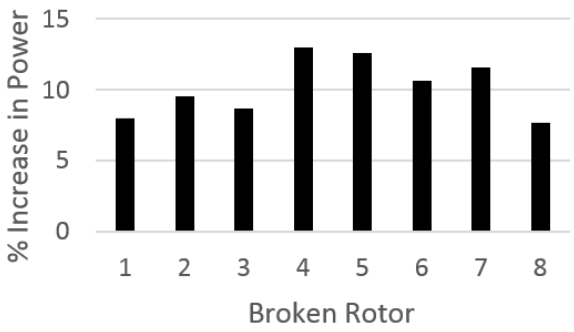

Fig. 12 Percent Change in Power with Broken Rotor

For the fully operational octocopter, the rear rotors generate more thrust than the front rotors, to maintain a nose-down attitude. When one of these rotors is lost, more thrust has to be redistributed to the remaining rotors. Thus, there is a tendency for rear rotor failure to cause greater increases in power consumption (compare rotors 4, 5, and 6 to rotors 1, 2, and 8 in Fig. 12). This is an extension of the trend observed for the hexacopter in [9], where only the front rotors were considered.

Comparing rotors that are equidistant from the pitch axis (rotors 2 and 8, 3 and 7, and 4 and 6) in Fig. 12, it is clear that failure in rotors 2, 4, and 7 causes a greater increase in overall power than does failure in rotors 8, 6, and 3. Comparing the yaw moments caused by rotors 3 and 7 (Fig. 13), there are two sources: the hub reaction torque (counter-clockwise for both rotors), and the drag-induced yaw moment (clockwise for rotor 3 and counterclockwise for rotor 7). On rotor 3, these two moments act in opposite directions, and partially cancel, while on rotor 7, they act in the same direction and sum together. Thus, loss of rotor 7 induces a greater yaw moment than rotor 3 failure, which requires greater compensatory effort, and higher power consumption. Similar arguments can be made comparing rotors 2 and 8 and 4 and 6.

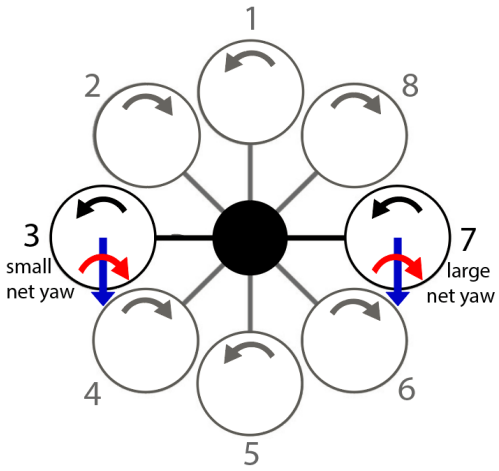

Fig. 13 Directions of Hub and Drag Yaw on Rotors 3 & 7 in Forward Flight

V. Conclusions

A dynamic simulation model of an octocopter based on the AeroQuad Cyclone ARF kit is presented and used to analyze the operation and performance of the aircraft in hover and forward flight at 10 m/s. The simulation model utilizes blade-element theory and a finite-state dynamic inflow model to represent the rotor induced velocity. This model is chosen in order to capture the rotor thrust and torque as well as the rotor in-plane forces (hub drag and side-force) and hub moments (rolling and pitching moments) at the flight speeds of interest. The aircraft is simulated in cases where all rotors are operational as well as in cases where a single rotor has failed, trim controls and aircraft power are calculated and analyzed.

The fully operational octocopter trims in hover by operating all eight rotors at identical speeds, a condition that requries 144 Watts to operate in. Once any single rotor fails, trim solutions exist for the aircraft that utilize the original reactionless multrotor controls for the aircraft to drive the thrust of the failed rotor to zero. The combination of reactionless controls used to re-trim the aircraft is dependent on the location of the failed rotor, only the original reactionless controls that command any change in thrust on the failed rotor are used, those that are used are utilized such that each contribution tends to drive the commanded thrust of the failed rotor toward zero. The power optimal trim solution for single rotor failure in hover requires 159 Watts, a 10.7% power penalty over the baseline aircraft.

In forward flight, the rotors produce net in-plane forces and hub moments. These effects, along with contributions from fuselage drag, noticeably change the trim solution from the hover case. At 10 m/s, the aft rotors spin faster than forward rotors in order to pitch the aircraft nose-down (to overcome drag) and produce a nose-down pitching moment to maintain zero acceleration for the aircraft. Rotor failure in this flight condition can not be generalized in the same way as hover, each rotor failure case is instead handled individually in analysis. Overall, rotor failure in forward flight is recovered in a similar manner to hover in terms of what original reactionless modes are used to restore aircraft equilibrium, but there are also small inputs of other multirotor controls, namely T_R and T_Y, to reconcile additional imbalances resulting from the loss of the failed rotor in-plane forces and hub moments. Because of the different magnitude of force and moment contributions from the non-unifrom trim controls, as well as the different directionality of the rotor hub moments and in-plane forces, the combination of multirotor controls used for a particular rotor varies case to case. These differences result in different power penalties for different rotor failures. Generally, aft rotor failure requires a larger increase in power than forward rotor failure, but there is also a larger penalty for rotors where the hub torque and in-plane force induced torque act in the same direction. Overall, the power penalty incurred in forward flight ranges from 7.7-13% depending on the rotor that has failed.

References

[1] Mueller, M. W., and D'Andrea, R., "Relaxed hover solutions for multicopters: Application to algorithmic redundancy and novel vehicles," *The International Journal of Robotics Research*, Vol. 35, No. 8, 2016, pp. 873–889. doi:10.1177/0278364915596233, URL `https://doi.org/10.1177/0278364915596233`.

[2] Falconí, G. P., and Holzapfel, F., "Adaptive Fault Tolerant Control Allocation for a Hexacopter System," *American Control Conference*, 2016, pp. 6760–6766. doi:10.1109/ACC.2016.7526736.

[3] Falconí, G. P., Angelov, J., and Holzapfel, F., "Hexacopter outdoor flight test results using adaptive control allocation subject to an unknown complete loss of one propeller," *2016 3rd Conference on Control and Fault-Tolerant Systems (SysTol)*, 2016, pp. 373–380. doi:10.1109/SYSTOL.2016.7739779.

[4] Schneider, T., Ducard, G., Konrad, R., and Pascal, S., "Fault-tolerant Control Allocation for Multirotor Helicopters Using Parametric Programming," *International Micro Air Vehicle Conference and Flight Competition (IMAV)*, Braunschweig, Germany, 2012. URL https://hal.archives-ouvertes.fr/hal-01302202.

[5] Achtelik, M., Doth, K.-M., Gurdan, D., and Strumpf, J., "Design of a Multi Rotor MAV with regard to Efficiency, Dynamics and Redundancy," *AIAA Guidance, Navigation, and Control Conference*, Reston, VA, 2012. URL https://doi.org/10.2514/6.2012-4779.

[6] Marks, A., Whidborne, J. F., and Yamamoto, I., "Control Allocation for Fault Tolerant Control of a VTOL Octorotor," *2012 UKACC International Conference on Control*, Cardiff, UK, 2012. doi:10.1109/CONTROL.2012.6334656.

[7] Niemiec, R., and Gandhi, F., "Effect on Inflow Model on Simulated Aeromechanics of a Quadrotor Helicopter," *72nd Annual Forum of the American Helicopter Society International*, Fairfax, VA, 2016.

[8] Peters, D., Boyd, D., and He, C., "Finite-State Induced-Flow Model for Rotors in Hover and Forward Flight," *43rd Annual Forum of the American Helicopter Society International*, Fairfax, VA, 1987.

[9] McKay, M., Niemiec, R., and Gandhi, F., "Control Reconfiguration for a Hexacopter Experiencing Single Rotor Failure," *Proceedings of the 27th International Conference on Adaptive Structures and Technologies*, Bolton Landing, NY, 2016.

[10] McKay, M., Niemiec, R., and Gandhi, F., "An Analysis of Classical and Alternate Hexacopter Configurations with Single Rotor Failure," *Journal of Aircraft*, Vol. 0, No. 0, 2018, pp. 1–8. doi:10.2514/1.C035005, URL http://arc.aiaa.org/doi/abs/10.2514/1.C035005.

[11] Niemiec, R., and Gandhi, F., "Multi-rotor Coordinate Transforms for Orthogonal Primary and Redundant Controls for Regular Hexacopters and Octocopters," *42nd European Rotorcraft Forum*, Paris, France, 2016.